HAL open science

A BOUNDARY-PARTITION-BASED DIAGRAM OF D-DIMENSIONAL BALLS: DEFINITION, PROPERTIES AND APPLICATIONS

Xianglong Duan, Chaoyu Quan, Benjamin Stamm

To cite this version:

Xianglong Duan, Chaoyu Quan, Benjamin Stamm. A BOUNDARY-PARTITION-BASED DIAGRAM OF D-DIMENSIONAL BALLS: DEFINITION, PROPERTIES AND APPLICATIONS. 2018. hal-01883443v1

HAL Id: hal-01883443

https://hal.science/hal-01883443v1

Preprint submitted on 28 Sep 2018 (v1), last revised 19 Oct 2019 (v2)

HAL is a multi-disciplinary open access archive for the deposit and dissemination of scientific research documents, whether they are published or not. The documents may come from teaching and research institutions in France or abroad, or from public or private research centers.

L'archive ouverte pluridisciplinaire **HAL**, est destinée au dépôt et à la diffusion de documents scientifiques de niveau recherche, publiés ou non, émanant des établissements d'enseignement et de recherche français ou étrangers, des laboratoires publics ou privés.

A VORONOI-TYPE DIAGRAM OF D-DIMENSIONAL BALLS: DEFINITION, PROPERTIES AND APPLICATIONS*

XIANGLONG DUAN†, CHAOYU QUAN‡, AND BENJAMIN STAMM§

Abstract. The power diagram, which is a partition of the Euclidean space, has been widely used, for example, to compute the volume of a union of d-dimensional balls (d-balls). In this article, an alternative partition is proposed, which is a generalized Voronoi diagram based on the boundary components of the union of d-balls in any dimension d. The definition, properties and applications of this new diagram are presented.

Key words. Voronoi diagram, power diagram, union of d-dimensional balls, medial axis

AMS subject classifications. 52C07

1. Introduction. The Voronoi diagram [9, 14] was initially a partition of the 2-dimensional (2D) plane into regions, based on the distance to points in a specific subset of the plane. In the general case, for a Euclidean subspace $X \subset \mathbb{E}^d$ (here, $\mathbb{E}^d$ represents the d-dimensional Euclidean space) endowed with a distance function and a tuple of nonempty subsets $\{A_i\}_{i\in K}$ in X, the Voronoi region $R_{\mathrm{v}}(A_i)$ associated with A_i is the set of all points in X whose distance to A_i is not greater than their distance to any other set A_j. In other words, the Voronoi region $R_{\mathrm{v}}(A_i)$ is given by

$$R_{\mathrm{v}}(A_i) = \{\mathbf{x} \in X \mid \mathrm{dist}(\mathbf{x}, A_i) \leq \mathrm{dist}(\mathbf{x}, A_j)\}\,, \tag{1.1}$$

where the distance function between a point $\mathbf{x}$ and a set A_i defined as

$$\mathrm{dist}(\mathbf{x}, A_i) \;\coloneqq\; \inf_{\mathbf{y}\in A_i} |\mathbf{x} - \mathbf{y}|. \tag{1.2}$$

Here, the notation $|\cdot|$ denotes the Euclidean norm and $\mathrm{dist}(\cdot,\cdot)$ is the Euclidean distance between a point and a set. Most commonly, each subset A_i is taken as a point and its corresponding Voronoi region $R_{\mathrm{v}}(A_i)$ is consequently a polyhedron, as depicted on the left of Figure 1 for a simple example in the plane.

In computational geometry, the power diagram [11, 3], also called the Laguerre-Voronoi diagram, is another partition of the 2D plane into polygonal cells with respect to a finite set of circles. In the general case, for a finite set of spheres $\{S_i\}_{i\in K}$ in $\mathbb{E}^d$ with $d \geq 2$ (which are circles in $\mathbb{E}^2$), the power region $R_{\mathrm{p}}(S_i)$ consists of all points whose power distances to S_i are not larger than their power distances to any other sphere S_j. The power distance from a point $\mathbf{x} \in \mathbb{E}^d$ to a sphere S_i with center $\mathbf{c}_i$ and radius r_i is defined as

$$\mathrm{dist}_{\mathrm{p}}(\mathbf{x}, S_i) \;\coloneqq\; \mathrm{dist}^2(\mathbf{x}, \mathbf{c}_i) - r_i^2. \tag{1.3}$$

The power region $R_{\mathrm{p}}(S_i)$ is then given by

$$R_{\mathrm{p}}(S_i) = \left\{\mathbf{x} \in \mathbb{E}^d \mid \mathrm{dist}_{\mathrm{p}}(\mathbf{x}, S_i) \leq \mathrm{dist}_{\mathrm{p}}(\mathbf{x}, S_j)\right\}. \tag{1.4}$$

*Preprint, 2018.

†Laboratoire de Mathématiques d'Orsay, Univ Paris-Sud 11, CNRS, Université Paris-Saclay, F-91405, Orsay, France (xianglong.duan@math.u-psud.fr).

‡Sorbonne Universités, UPMC Univ Paris 06, Institut des Sciences du Calcul et des Données (ISCD), F-75005, Paris, France (chaoyu.quan@upmc.fr).

§Center for Computational Engineering Science, RWTH Aachen University, Aachen, Germany (best@mathcces.rwth-aachen.de).

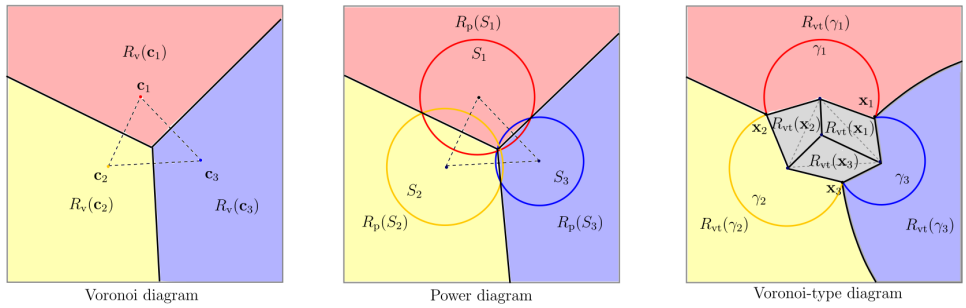

FIG. 1. *Left: Voronoi diagram of three points; middle: the power diagram of three circles; right: Voronoi-type diagram of the same circles as in the power diagram.*

The power diagram can be seen as a generalized Voronoi diagram, in the sense that one can simply replace the distance function $\mathrm{dist}(\cdot,\cdot)$ in Eq. (1.1) with the power distance function $\mathrm{dist}_{\rm p}(\cdot,\cdot)$. Figure 1 gives an example of three circles in the plane. Note that the power distance here is not a real distance function. The volume of the union of balls can be computed by summing up the volume of each power cell inside the union [4, 7]. Each power cell is characterized as the corresponding ball cut by (hyper)planes.

In this article, we propose a new Voronoi-type diagram of d-dimensional balls (d-balls) in $\mathbb{E}^d$, based on the different components of the boundary of the union of these d-balls. This diagram is an alternative to the power diagram and can also be seen as a generalized Voronoi diagram. For example, on the right-hand side of Figure 1, there exists three intersected discs in plane, whose boundary is composed of open circular arcs $\{\gamma_1,\gamma_2,\gamma_3\}$ and intersection points $\{\mathbf{x}_1,\mathbf{x}_2,\mathbf{x}_3\}$. We take the sets $\{A_i\}$ introduced for the Voronoi diagram as $\{\gamma_1,\gamma_2,\gamma_3,\mathbf{x}_1,\mathbf{x}_2,\mathbf{x}_3\}$, to obtain six corresponding regions from Eq. (1.1). This gives a new partition of the plane, in particular, a new partition of the union of the discs including circular sectors and polygons. Further, this Voronoi-type diagram can be generalized to any dimension $d\geq 2$ as explained briefly in the following.

In the general case, the boundary of the union of d-balls can be classified into a list of spherical patches

$$\left\{\gamma_i^{(k)}\right\}_{0\leq k\leq d-1,\ 1\leq i\leq n_k} \tag{1.5}$$

where k denotes the dimension of the patch and n_k is the number of k-dimensional patches (k-patches). More details about this classification will be presented in Section 2.1. In particular, a 0-patch represents an intersection point and a 1-patch presents an open circular arc or a circle. Similar to the 2D case, we can define the Voronoi-type diagram of these d-balls, where the Voronoi-type cell corresponding to $\gamma_i^{(k)}$ is given by

$$R_{\rm vt}(\gamma_i^{(k)}) = \left\{\mathbf{x}\in\mathbb{E}^d \mid \mathrm{dist}(\mathbf{x},\gamma_i^{(k)})\leq \mathrm{dist}(\mathbf{x},\gamma_j^{(l)})\right\}, \tag{1.6}$$

where the distance function $\mathrm{dist}(\cdot,\cdot)$ is given by Eq. (1.2). We mention that this Voronoi-type diagram was first proposed by some of us to characterize smooth molecular surfaces in $\mathbb{E}^3$, see [16] for details.

In Section 2, we first study the properties of the Voronoi-type cells, based on analyzing the signed distance from an arbitrary point to the boundary of the union of

d-balls. Then, in Section 3, we present how this diagram can be used to compute the volume of the union of d-balls. In Section 4, we mention its application to characterize the smooth molecular surface in $\mathbb{E}^3$. After that, in Section 5, we introduce briefly its application to compute the medial axis of the union of balls. Finally, we draw some conclusions.

2. Voronoi-type diagram. We consider a finite set of $(d-1)$-dimensional spheres $\{S_1, S_2, \ldots, S_N\}$ in $\mathbb{E}^d$, where the d-sphere S_i has center $\mathbf{c}_i \in \mathbb{E}^d$ and radius r_i for each $1 \leq i \leq N$. The corresponding d-balls are consequently denoted by $\{B_1, B_2, \ldots, B_N\}$ where $B_i = B(\mathbf{c}_i, r_i)$. In this article, the notation $B(\mathbf{c}, r)$ denotes the open ball with center $\mathbf{c}$ and radius r. The union of these d-balls is denoted by Ω, that is,

$$\Omega := \bigcup_{i=1}^{N} B_i \tag{2.1}$$

and the boundary of this union is denoted by $\Gamma := \partial\Omega$. The open region on the outside of Ω is denoted by $\overline{\Omega}^{\mathsf{c}} := \mathbb{E}^d \setminus (\Omega \cup \Gamma)$.

Since the boundary Γ is a closed and compact set, for any point $\mathbf{p} \in \mathbb{E}^d$, there exists at least one closest point in Γ to $\mathbf{p}$. The signed distance function f_Γ with respect to Γ is then given as follows

$$f_\Gamma(\mathbf{p}) := \begin{cases} -\mathrm{dist}(\mathbf{p}, \Gamma) & \text{if } \mathbf{p} \in \Omega, \\ \mathrm{dist}(\mathbf{p}, \Gamma) & \text{if } \mathbf{p} \in \Omega^{\mathsf{c}} \ . \end{cases} \tag{2.2}$$

As a consequence, the three sets Ω, Γ and $\overline{\Omega}^{\mathsf{c}}$ can be mathematically characterized by $\Omega = \{\mathbf{p} \mid f_\Gamma(\mathbf{p}) < 0\}$, $\Gamma = \{\mathbf{p} \mid f_\Gamma(\mathbf{p}) = 0\}$ and $\overline{\Omega}^{\mathsf{c}} = \{\mathbf{p} \mid f_\Gamma(\mathbf{p}) > 0\}$.

Remark 2.1. Another way to characterize Ω, Γ and $\overline{\Omega}^{\mathsf{c}}$ is to use the notion of the local signed distance functions $f_i(\mathbf{p})$ to S_i, defined by $f_i(\mathbf{p}) = |\mathbf{p} - \mathbf{c}_i| - r_i$, $\forall \mathbf{p} \in \mathbb{E}^d$ and $1 \leq i \leq N$. By defining the following function

$$F(\mathbf{p}) := \min_{1 \leq i \leq N} \{f_i(\mathbf{x})\}, \tag{2.3}$$

the sets Ω, Γ and $\overline{\Omega}^{\mathsf{c}}$ can also be characterized by $\Omega = \{\mathbf{p} \mid F(\mathbf{p}) < 0\}$, $\Gamma = \{\mathbf{p} \mid F(\mathbf{p}) = 0\}$ and $\overline{\Omega}^{\mathsf{c}} = \{\mathbf{p} \mid F(\mathbf{p}) > 0\}$.

2.1. Characterization of the boundary. As mentioned previously, the boundary Γ is composed of spherical patches of different dimensions from 0 to $d-1$. We will provide more details in this subsection.

We first define a mapping $\mathcal{I}$ as follows

$$\mathbf{x} \in \Gamma \mapsto \mathcal{I}(\mathbf{x}) := \{i_1, i_2, \ldots, i_m \mid \mathbf{x} \in S_{i_t},\ t = 1, \ldots, m\} \subseteq \{1, 2, \ldots, N\}, \tag{2.4}$$

where $\mathcal{I}(\mathbf{x})$ collects all indices of the spheres containing $\mathbf{x}$ and m is the number of these spheres. Then, we can define the intersection set of these spheres as follows

$$S_{\mathbf{i}} := \bigcap_{t=1}^{m} S_{i_t}, \tag{2.5}$$

where the subscript $\mathbf{i} = \mathcal{I}(\mathbf{x}) = \{i_1, i_2, \ldots, i_m\}$ depends on $\mathbf{x}$, see an example in Figure 2. Further, the affine space generated by the associated centers

$$\mathbf{c}_{\mathbf{i}} := \{\mathbf{c}_{i_1}, \mathbf{c}_{i_2}, \ldots, \mathbf{c}_{i_m}\} \tag{2.6}$$

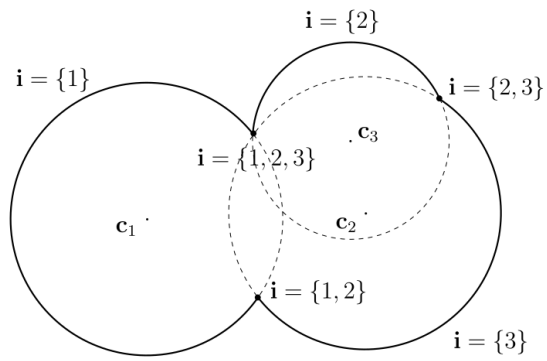

FIG. 2. *2D schematic diagram of the index set* $\mathbf{i} = \mathcal{I}(\mathbf{x})$ *at the boundary of three discs.*

is denoted by

$$\Lambda_{\mathbf{i}} := \{\mathbf{y} \mid \mathbf{y} = \sum_{t=1}^{m} \lambda_t \mathbf{c}_{i_t},\ \sum_{t=1}^{m} \lambda_t = 1,\ \lambda_t \in \mathbb{R}\}. \tag{2.7}$$

With the above notations, we propose the following lemma.

LEMMA 2.2. *In the case when* $S_{\mathbf{i}}$ *is non-empty and* $\dim(\Lambda_{\mathbf{i}}) \leq d-1$, $S_{\mathbf{i}}$ *is either a* k*-dimensional sphere (*k*-sphere) with*

$$k = \dim(S_{\mathbf{i}}) = d - \dim(\Lambda_{\mathbf{i}}) - 1, \tag{2.8}$$

or a point (the degenerate case), where $\dim(\cdot)$ *denotes the dimension. In the case when* $S_{\mathbf{i}}$ *is non-empty and* $\dim(\Lambda_{\mathbf{i}}) = d$, $S_{\mathbf{i}}$ *is a point.*

Proof. Let's take an arbitrary point $\mathbf{x}_0 \in S_{\mathbf{i}}$. We rewrite $S_{\mathbf{i}}$ in the following form

$$\begin{aligned} S_{\mathbf{i}} &= \{\mathbf{x} \mid |\mathbf{x} - \mathbf{c}_{i_t}|^2 - |\mathbf{x}_0 - \mathbf{c}_{i_t}|^2 = 0,\ 1 \leq t \leq m\} \\ &= S_{i_1} \cap P_{\mathbf{i}}, \end{aligned} \tag{2.9}$$

where

$$\begin{aligned} P_{\mathbf{i}} &= \{\mathbf{x} \mid |\mathbf{x} - \mathbf{c}_{i_t}|^2 - |\mathbf{x}_0 - \mathbf{c}_{i_t}|^2 = |\mathbf{x} - \mathbf{c}_{i_1}|^2 - |\mathbf{x}_0 - \mathbf{c}_{i_1}|^2,\ 2 \leq t \leq m\} \\ &= \{\mathbf{x} \mid (\mathbf{x} - \mathbf{x}_0, \mathbf{c}_{i_t} - \mathbf{c}_{i_1}) = 0,\ 2 \leq t \leq m\}. \end{aligned} \tag{2.10}$$

Here, $P_{\mathbf{i}}$ is the intersection of $m-1$ hyperplanes that contain $\mathbf{x}_0$. It is an affine space with $\dim(P_{\mathbf{i}}) = d - \dim(\Lambda_{\mathbf{i}})$ and satisfies $P_{\mathbf{i}} - \mathbf{x}_0 \perp \Lambda_{\mathbf{i}} - \mathbf{c}_{i_1}$.

In the case of $\dim(\Lambda_{\mathbf{i}}) \leq d-1$, we then have $\dim(P_{\mathbf{i}}) \geq 1$. Note that $S_{\mathbf{i}}$ is the intersection of the sphere S_{i_1} and the affine space $P_{\mathbf{i}}$. If $S_{\mathbf{i}}$ is non-empty, then it is either a sphere with $\dim(S_{\mathbf{i}}) = d - \dim(\Lambda_{\mathbf{i}}) - 1$, or a single point in the degenerate case when $P_{\mathbf{i}}$ is tangent to $S_{\mathbf{i}}$. We mention that in this degenerate case, $S_{\mathbf{i}}$ is a point contained in $\Lambda_{\mathbf{i}}$ with $\dim(\Lambda_{\mathbf{i}}) \leq d-1$. Furthermore, in the case of $\dim(\Lambda_{\mathbf{i}}) = d$, we have $\dim(P_{\mathbf{i}}) = 0$ and $P_{\mathbf{i}}$ is consequently the point $\mathbf{x}_0$. If $S_{\mathbf{i}}$ is nonempty, then $S_{\mathbf{i}}$ is just the point $\mathbf{x}_0$. ∎

For a given set of indices $\mathbf{i} \subseteq \{1, 2, \ldots, N\}$, if $\dim(S_{\mathbf{i}}) \geq 1$, we can define the following set

$$\Gamma_{\mathbf{i}} := \{\mathbf{x} \in \Gamma \mid \mathcal{I}(\mathbf{x}) = \mathbf{i}\} \subseteq S_{\mathbf{i}} \cap \Gamma, \tag{2.11}$$

which is open in $S_{\mathbf{i}}$. In this case, we can further divide $\Gamma_{\mathbf{i}}$ as follows

$$\Gamma_{\mathbf{i}} = \bigcup_j \gamma_{\mathbf{i},j}^{(k)}, \tag{2.12}$$

where $\gamma_{\mathbf{i},j}^{(k)} \subseteq \Gamma_{\mathbf{i}}$ is an open connected k-patch and $k = \dim(S_{\mathbf{i}}) = \dim(\gamma_{\mathbf{i},j}^{(k)})$ denotes the dimension. This means that $\Gamma_{\mathbf{i}}$ has been divided into different k-patches. For the sake of simplicity, we can reorder all patches $\{\gamma_{\mathbf{i},j}^{(k)}\}$ based on the dimension k, by replacing the subscripts $(\mathbf{i}, j)$ with only one subscript i. As a consequence, the whole boundary Γ is classified into a set of patches $\{\gamma_i^{(k)}\}$ with $0 \le k \le d-1,\ 1 \le i \le n_k$, that is,

$$\Gamma = \bigcup_{k=0}^{d-1} \bigcup_{i=1}^{n_k} \gamma_i^{(k)}, \tag{2.13}$$

where n_k is the number of k-patches and $\gamma_i^{(k)}$ is an open connected k-patch when $k \ge 1$. In particular, $\gamma_i^{(0)}$ is simply an intersection point and $\gamma_i^{(1)}$ is a circular arc or a circle. From the derivation of $\gamma_i^{(k)}$, we know that $\mathcal{I}(\mathbf{x})$ holds the same for any point $\mathbf{x} \in \gamma_i^{(k)}$. Therefore, we can generalize the definition of $\mathcal{I}$ as follows

$$\mathcal{I}(\gamma_i^{(k)}) := \mathcal{I}(\mathbf{x}), \tag{2.14}$$

where $\mathbf{x} \in \gamma_i^{(k)}$ is an arbitrary point on $\gamma_i^{(k)}$.

Next, we analyze the signed distance f_Γ to the boundary Γ, which involves in finding one closest point to any given point $\mathbf{p}$ (note that the uniqueness of the closest point is not guaranteed).

2.2. Analysis of the signed distance. We want to analyze the signed distance from an arbitrary point to the boundary Γ of the union of d-balls. We first consider the case when the point lies outside the union and give the following lemma. The proof of this lemma is trivial and therefore skipped here.

LEMMA 2.3. *For any point* $\mathbf{p} \in \overline{\Omega}^{\mathsf{c}}$, $\operatorname{dist}(\mathbf{p}, \Gamma) = F(\mathbf{p})$.

We now focus our attention to the case when $\mathbf{p} \in \overline{\Omega}$. In fact, this case is studied from another aspect, in the sense that for any point $\mathbf{x}$ on Γ, we study the set of all points in $\overline{\Omega}$ that treat $\mathbf{x}$ as a closest point on Γ. We define a mapping $\mathcal{R}$ such that $\forall \mathbf{x} \in \Gamma$,

$$\mathcal{R}(\mathbf{x}) = \{\mathbf{p} \in \overline{\Omega} \mid \operatorname{dist}(\mathbf{p}, \Gamma) = |\mathbf{p} - \mathbf{x}|\} \subseteq \overline{\Omega}, \tag{2.15}$$

which represents the region consisting of the points having $\mathbf{x}$ as a closest point. The convexity of the set $\mathcal{R}(\mathbf{x})$ is ensured according to the following lemma.

LEMMA 2.4. $\forall \mathbf{x} \in \Gamma$, *the set* $\mathcal{R}(\mathbf{x})$ *is convex. Further, it holds that* $\operatorname{conv}(\mathbf{x}, \mathbf{c}_{\mathbf{i}}) \subseteq \mathcal{R}(\mathbf{x})$, *where* $\mathbf{i} = \mathcal{I}(\mathbf{x}) = \{i_1, i_2, \ldots, i_m\}$. *Here, the notation* conv *denotes the convex hull of a set of points.*

Proof. We first need to prove that $\forall \mathbf{p}_1, \mathbf{p}_2 \in \mathcal{R}(\mathbf{x})$ and $\forall \lambda \in [0,1]$, $\mathbf{p}_0 = \lambda \mathbf{p}_1 + (1-\lambda)\mathbf{p}_2 \in \mathcal{R}(\mathbf{x})$. To do this, we construct a function as follows

$$h(\mathbf{p}) = \operatorname{dist}(\mathbf{p}, \Gamma)^2 - |\mathbf{p} - \mathbf{x}|^2 = \inf_{\mathbf{y} \in \Gamma} \left\{2(\mathbf{x} - \mathbf{y}) \cdot \mathbf{p} + |\mathbf{y}|^2 - |\mathbf{x}|^2\right\}, \qquad \mathbf{p} \in \mathbb{E}^d. \tag{2.16}$$

As a consequence, $\mathbf{x}$ is a closest point on Γ to $\mathbf{p}$ if and only if $h(\mathbf{p}) = 0$. As an obvious fact, we have $h(\mathbf{p}) \leq 0,\ \forall \mathbf{p} \in \mathbb{E}^d$. Since $\mathbf{x}$ is a closest point on Γ to $\mathbf{p}_1$ and to $\mathbf{p}_2$, we have $h(\mathbf{p}_1) = h(\mathbf{p}_2) = 0$. Then, we can compute

$$\begin{aligned} h(\mathbf{p}_0) &= \inf_{\mathbf{y}\in\Gamma} \left\{2(\mathbf{x}-\mathbf{y})\cdot\left[\lambda\mathbf{p}_1 + (1-\lambda)\mathbf{p}_2\right] + |\mathbf{y}|^2 - |\mathbf{x}|^2\right\} \\ &\geq \lambda \inf_{\mathbf{y}\in\Gamma} \left\{2(\mathbf{x}-\mathbf{y})\cdot\mathbf{p}_1 + |\mathbf{y}|^2 - |\mathbf{x}|^2\right\} \\ &\quad +(1-\lambda) \inf_{\mathbf{y}\in\Gamma} \left\{2(\mathbf{x}-\mathbf{y})\cdot\mathbf{p}_2 + |\mathbf{y}|^2 - |\mathbf{x}|^2\right\} \\ &= \lambda h(\mathbf{p}_1) + (1-\lambda) h(\mathbf{p}_2) \\ &= 0. \end{aligned} \tag{2.17}$$

□

This means that $\mathbf{x}$ is also a closest point to $\mathbf{p}_0$. To prove that $\mathbf{p} \in \mathcal{R}(\mathbf{x})$, we should show further that $\mathbf{p}_0 \in \overline{\Omega}$. As $\mathbf{x}$ is a closest point to $\mathbf{p}_1$, we know that the ball centered at $\mathbf{p}_1$ with radius $|\mathbf{p}_1 - \mathbf{x}|$ is covered by $\overline{\Omega}$, i.e.,

$$B(\mathbf{p}_1, |\mathbf{p}_1 - \mathbf{x}|) \subseteq \overline{\Omega}.$$

Similarly, we have $B(\mathbf{p}_2, |\mathbf{p}_2 - \mathbf{x}|) \subseteq \overline{\Omega}$. Notice that the line segment $\overline{\mathbf{p}_1\mathbf{p}_2}$ is covered by the union of these two balls (intersecting at $\mathbf{x}$), which implies that $\mathbf{p}_0 \in \overline{\mathbf{p}_1\mathbf{p}_2} \subseteq \overline{\Omega}$. Since $\mathbf{p}_0$ has $\mathbf{x}$ as a closest point and $\mathbf{p}_0 \in \overline{\Omega}$, we therefore have $\mathbf{p}_0 \in \mathcal{R}(\mathbf{x})$. So far, we have proved that $\mathcal{R}(\mathbf{x})$ is convex.

Further, if there exists a set of spheres $\{S_{i_t}\}_{t=1,\ldots,m}$ each containing $\mathbf{x} \in \Gamma$, it is obvious that $\mathbf{x}$ is a closest point of $\mathbf{c}_{i_t}$. In addition, we know that $\mathbf{x} \in \Gamma$ is a closest point to itself. Due to the convexity of $\mathcal{R}(\mathbf{x})$, we then have $\mathrm{conv}(\mathbf{x}, \mathbf{c}_{\mathbf{i}}) \subseteq \mathcal{R}(\mathbf{x})$.

THEOREM 2.5. *Given a point* $\mathbf{x} \in \Gamma$ *and* $\mathbf{i} = \mathcal{I}(\mathbf{x}) = \{i_1, i_2, \ldots, i_m\}$*, the following statements hold:*

(1) $\mathcal{R}(\mathbf{x}) \subseteq \mathrm{cone}(\mathbf{x}; \mathbf{v}_1, \mathbf{v}_2, \ldots, \mathbf{v}_m)$*, where* $\mathbf{v}_t := \mathbf{c}_{i_t} - \mathbf{x}$ *and* $\mathrm{cone}(\mathbf{x}; \mathbf{v}_1, \mathbf{v}_2, \ldots, \mathbf{v}_m) = \{\mathbf{y} \mid \mathbf{y} = \mathbf{x} + \sum_{t=1}^{m} \lambda_t \mathbf{v}_t,\ \lambda_t \geq 0,\ 1 \leq t \leq m\}$ *represents a convex cone (as in linear algebra) with apex* $\mathbf{x}$*.*

(2) *If there exists another point* $\mathbf{x}' \in \Gamma$ *satisfying* $\mathbf{x}' \neq \mathbf{x}$ *and* $\mathbf{x}' \in S_{\mathbf{i}}$*, then* $\mathcal{R}(\mathbf{x}) = \mathrm{conv}(\mathbf{x}, \mathbf{c}_{\mathbf{i}})$*.*

Proof. (1) According to Theorem 19.1 in the book [17], we can write

$$\mathrm{cone}(\mathbf{x}; \mathbf{v}_1, \mathbf{v}_2, \ldots, \mathbf{v}_m) = \bigcap_{s=1}^{N_0} H_s, \tag{2.18}$$

where $H_s := \{\mathbf{y} \mid (\mathbf{y}, \mathbf{n}_s) \leq b_s\}$ is a half-space in $\mathbb{E}^d$, $\mathbf{n}_s$ denotes its normal vector, $b_s = (\mathbf{x}, \mathbf{n}_s)$ is a real number, N_0 denotes the number of half-spaces and $(\cdot,\cdot)$ denotes the Euclidean scalar product in $\mathbb{E}^d$. Each half-space H_s corresponds to a hyperplane P_s defined by

$$P_s := \{\mathbf{y} \mid (\mathbf{y}, \mathbf{n}_s) = b_s\}.$$

Without loss of generality, we suppose that $|\mathbf{n}_s| = 1$ for each half-space H_s. Furthermore, each hyperplane P_s is supposed to contain at least one ray starting from $\mathbf{x}$ in a direction among $\{\mathbf{v}_1, \mathbf{v}_2, \ldots, \mathbf{v}_m\}$. In fact, the half-space H_s can be removed in Eq. (2.18) if P_s does not contains any such ray. To prove the first statement of the theorem, it suffices to show that $\forall \mathbf{p} \in \mathcal{R}(\mathbf{x})$ and $1 \leq s \leq N_0$, it follows that $\mathbf{p} \in H_s$.

Let $\mathbf{p} \in \mathcal{R}(\mathbf{x})$ and s be fixed. As mentioned above, P_s contains a ray starting from $\mathbf{x}$ in direction $\mathbf{v}_r,\ 1 \le r \le m$. Then, we have $(\mathbf{x} + \lambda \mathbf{v}_r, \mathbf{n}_s) = b_s,\ \forall \lambda \ge 0$, which implies that $(\mathbf{v}_r, \mathbf{n}_s) = 0$.

We now construct a small curve $\zeta_s(x)$ starting from $\mathbf{x}$ and lying on Γ in the direction of $\mathbf{n}_s$, of the form

$$\zeta_s(x) = \mathbf{x} + x\mathbf{n}_s + \alpha(x)\mathbf{v}, \qquad x \in [0, \varepsilon], \tag{2.19}$$

where $\alpha(x) \ge 0$ is a function with respect to x satisfying $\alpha(0) = 0$, $\mathbf{v}$ is a nonzero vector in $\mathbb{E}^d$ and ε is a sufficiently small positive number. In order to choose $\mathbf{v}$, we define the following nonempty set

$$\mathcal{A}_s = \{\mathbf{v}_t \mid (\mathbf{v}_t, \mathbf{n}_s) = 0,\ 1 \le t \le m\} \ni \mathbf{v}_r.$$

As a consequence, the vector $\mathbf{v}$ and the function $\alpha(x)$ can be constructed as follows

$$\mathbf{v} = c_s \mathbf{v}_r, \tag{2.20}$$

and

$$\alpha(x) = 1 - \sqrt{1 - \frac{x^2}{|\mathbf{v}|^2}} \in [0, 1], \qquad 0 \le x \le |\mathbf{v}|, \tag{2.21}$$

where $c_s = \max\limits_{\mathbf{v}_t \in \mathcal{A}_s} \dfrac{(\mathbf{v}_t, \mathbf{v}_r)}{|\mathbf{v}_r|^2} = \dfrac{(\mathbf{v}_{t_0}, \mathbf{v}_r)}{|\mathbf{v}_r|^2} \ge 1$ for some $\mathbf{v}_{t_0} \in \mathcal{A}_s$. The above-constructed $\mathbf{v}$ has the following two properties

$$(\mathbf{v}, \mathbf{v} - \mathbf{v}_{t_0}) = (\mathbf{v}, \mathbf{v}) - (\mathbf{v}, \mathbf{v}_{t_0}) = \frac{(\mathbf{v}_{t_0}, \mathbf{v}_r)^2}{|\mathbf{v}_r|^2} - \frac{(\mathbf{v}_{t_0}, \mathbf{v}_r)^2}{|\mathbf{v}_r|^2} = 0 \tag{2.22}$$

and

$$(\mathbf{v}, \mathbf{v} - \mathbf{v}_t) = \frac{(\mathbf{v}_{t_0}, \mathbf{v}_r)^2}{|\mathbf{v}_r|^2} - \frac{(\mathbf{v}_{t_0}, \mathbf{v}_r)(\mathbf{v}_t, \mathbf{v}_r)}{|\mathbf{v}_r|^2} \ge 0, \qquad \forall \mathbf{v}_t \in \mathcal{A}_s. \tag{2.23}$$

With the above construction of $\zeta_s(x)$ and the properties of $\mathbf{v}$, we can now state the following claim.

Claim 2.6. *$\exists\ \varepsilon > 0$, s.t., $\zeta_s(x) \in \Gamma,\ \forall x \in [0, \varepsilon]$.*

The proof of this claim is presented in Appendix A. Let's focus on the proof of the first statement in Theorem 2.5. For any point $\mathbf{p} \in \mathcal{R}(\mathbf{x})$, we know that $\mathbf{x}$ is a closest point on Γ to $\mathbf{p}$ and $\zeta_s(x) \in \Gamma,\ \forall x \in [0, \varepsilon]$. Therefore, we have

$$\frac{\mathrm{d}}{\mathrm{d}x}\big(|\zeta_s(x) - \mathbf{p}|^2\big)|_{x=0} \ge 0, \tag{2.24}$$

which yields that $(\mathbf{x} - \mathbf{p}, \zeta_s'(0)) \ge 0$. It is not difficult to find that $\zeta_s'(0) = \mathbf{n}_s$ and we then obtain $(\mathbf{p}, \mathbf{n}_s) \le (\mathbf{x}, \mathbf{n}_s) = b_s$. This implies that $\mathbf{p} \in H_s$ for each subscript s. The proof of the first statement in the theorem is complete.

(2) We now prove the second statement in Theorem 2.5. Suppose that there exists another point $\mathbf{x}' \in \Gamma$ such that $\mathbf{x}' \ne \mathbf{x}$ and $\mathbf{x}' \in S_{i_t},\ \forall 1 \le t \le m$. According to Lemma 2.4, we only need to prove that $\mathcal{R}(\mathbf{x}) \subseteq \mathrm{conv}(\mathbf{x}, \mathbf{c_i})$. For any point $\mathbf{p} \in \mathcal{R}(\mathbf{x})$, since

$\mathcal{R}(\mathbf{x}) \subseteq \mathrm{cone}(\mathbf{x}; \mathbf{v}_1, \mathbf{v}_2, \ldots, \mathbf{v}_m)$ from the first statement, there exist a set of positive numbers $\lambda_t \geq 0$, s.t.,

$$\mathbf{p} = \mathbf{x} + \sum_{t=1}^{m} \lambda_t \mathbf{v}_t.$$

Since $\mathbf{x}, \mathbf{x}' \in S_{i_t}$ for each $1 \leq t \leq m$, we have

$$0 = |\mathbf{x} - \mathbf{c}_{i_t}|^2 - |\mathbf{x}' - \mathbf{c}_{i_t}|^2 = -|\mathbf{x}' - \mathbf{x}|^2 + 2(\mathbf{x}' - \mathbf{x}) \cdot \mathbf{v}_t,$$

which yields that

$$2(\mathbf{x}' - \mathbf{x}) \cdot \mathbf{v}_t = |\mathbf{x} - \mathbf{x}'|^2, \qquad 1 \leq t \leq m.$$

Furthermore, since $\mathbf{x}$ is a closest point on Γ to $\mathbf{p}$, we have

$$|\mathbf{p} - \mathbf{x}|^2 \leq |\mathbf{p} - \mathbf{x}'|^2 = |\mathbf{p} - \mathbf{x}|^2 + 2(\mathbf{p} - \mathbf{x}) \cdot (\mathbf{x} - \mathbf{x}') + |\mathbf{x} - \mathbf{x}'|^2,$$

and therefore,

$$\begin{aligned} |\mathbf{x} - \mathbf{x}'|^2 &\geq 2(\mathbf{x}' - \mathbf{x}) \cdot (\mathbf{p} - \mathbf{x}) \\ &= 2 \sum_{t=1}^{m} \lambda_t (\mathbf{x}' - \mathbf{x}) \cdot \mathbf{v}_t \\ &= \left(\sum_{t=1}^{m} \lambda_t \right) |\mathbf{x} - \mathbf{x}'|^2. \end{aligned}$$

Since $\mathbf{x}' \neq \mathbf{x}$, we consequently have the inequality

$$\sum_{t=1}^{m} \lambda_t \leq 1,$$

which means that $\mathbf{p} \in \mathrm{conv}(\mathbf{x}, \mathbf{c_i})$. Then, we have $\mathcal{R}(\mathbf{x}) \subseteq \mathrm{conv}(\mathbf{x}, \mathbf{c_i})$. ∎

Corollary 2.7. *For each boundary component $\gamma_i^{(k)}$ of Γ, if $k \geq 1$, then $\forall \mathbf{x} \in \gamma_i^{(k)}$, $\mathcal{R}(\mathbf{x}) = \mathrm{conv}(\mathbf{x}, \mathbf{c_i})$, where $\mathbf{i} = \mathcal{I}(\gamma_i^{(k)}) = \{i_1, i_2, \ldots, i_m\}$.*

Proof. In the case of $k \geq 1$, $\gamma_i^{(k)}$ contains infinitely many points, each of which is contained and only contained by the set of spheres $\{S_{i_1}, S_{i_2}, \ldots, S_{i_m}\}$. Therefore, the second statement in Theorem 2.5 can be applied. ∎

2.3. Partition of the union of d-balls. In the introduction, we have introduced the concept of the Voronoi-type diagram in Eq. (1.6), which gives a partition of $\mathbb{E}^d$. According to Lemma 2.3, the partition of $\overline{\Omega}^{\mathsf{c}}$ is directly based on the simple function $F(\cdot)$ given by Eq. (2.3). Alternatively, one can also decompose $\overline{\Omega}^{\mathsf{c}}$ using the power distance or even simply treat $\overline{\Omega}^{\mathsf{c}}$ as one entire cell. Thus, in this section, we are only interested in the partition of $\overline{\Omega}$.

The mapping $\mathcal{R}$ maps any point $\mathbf{x} \in \Gamma$ to a subregion of $\overline{\Omega}$ that collects all points having $\mathbf{x}$ as a closest point. We now generalize the definition (2.15) of $\mathcal{R}$ as follows

$$\mathcal{R}(\gamma) = \bigcup_{\mathbf{x} \in \gamma} \mathcal{R}(\mathbf{x}) \subseteq \overline{\Omega}, \qquad \forall \gamma \subseteq \Gamma, \tag{2.25}$$

which maps any subset γ of Γ to a subregion of $\overline{\Omega}$ such that each point in the subregion has a closest point in γ. As a consequence, each Voronoi-type cell $R_{\mathrm{vt}}(\gamma_i^{(k)})$ (appearing in Eq. (1.6)) satisfies the following relationship

$$R_{\mathrm{vt}}(\gamma_i^{(k)}) \cap \overline{\Omega} = \mathcal{R}(\gamma_i^{(k)}), \qquad \forall 0 \leq k \leq d-1,\ 1 \leq i \leq n_k. \tag{2.26}$$

According to Theorem 2.5 and Corollary 2.7, in the case of $1 \le k \le d-1$, $\mathcal{R}(\gamma_i^{(k)})$ can be characterized by

$$\mathcal{R}(\gamma_i^{(k)}) = \bigcup_{\mathbf{x}\in\gamma_i^{(k)}} \mathrm{conv}(\mathbf{x}, \mathbf{c_i}), \qquad \forall 1 \le k \le d-1,\ 1 \le i \le n_k, \tag{2.27}$$

where $\mathbf{i} = \mathcal{I}(\gamma_i^{(k)})$. In the case of $k = 0$, $\gamma_i^{(0)}$ is an intersection point (0-patch). Then, according to the first statement in Theorem 2.5, we have

$$\mathrm{conv}(\gamma_i^{(0)}, \mathbf{c_i}) \subseteq \mathcal{R}(\gamma_i^{(0)}) \subseteq \mathrm{cone}(\gamma_i^{(0)}; \mathbf{v}_1, \mathbf{v}_2, \ldots, \mathbf{v}_m), \tag{2.28}$$

where $\mathbf{i} = \mathcal{I}(\gamma_i^{(0)}) = \{i_1, i_2, \ldots, i_m\}$ and $\mathbf{v}_t = \mathbf{c}_t - \gamma_i^{(0)}$ with $1 \le t \le m$.

To better understand the cell $\mathcal{R}(\gamma_i^{(0)})$, we define the following subregion of $\overline{\Omega}$ by

$$R_0 := \bigcup_{i=1}^{n_0} \mathcal{R}(\gamma_i^{(0)}). \tag{2.29}$$

Suppose that the classical Voronoi diagram of all intersection points $\{\gamma_i^{(0)}\}_{1\le i\le n_0}$ is given, which divides $\mathbb{R}^3$ into different Voronoi cells. The Voronoi cell corresponding to $\gamma_i^{(0)}$ is denoted by $\mathrm{Vor}\left(\gamma_i^{(0)}\right)$. As a consequence, the cell $\mathcal{R}(\gamma_i^{(0)})$ can be written as

$$\mathcal{R}(\gamma_i^{(0)}) = R_0 \cap \mathrm{Vor}\left(\gamma_i^{(0)}\right), \qquad 1 \le i \le n_0. \tag{2.30}$$

R_0 will be further analyzed later in Section 3.

Here, we provide two examples of the Voronoi-type partition. Figure 3 provides a partition of some discs in $\mathbb{E}^2$, respectively obtained from the power diagram (computed by F. McCollum's package) and the proposed Voronoi-type diagram. In the Voronoi-type diagram, the union of these discs is divided into circular sectors (in blue) and polygons (in red). The polygons constitute R_0, while the specific Voronoi-type cells $\{\mathcal{R}(\gamma_i^{(0)})\}$ are not illustrated. Figure 4 provides an example of the Voronoi-type diagram of three intersected balls in $\mathbb{E}^3$. The union of these 3-balls is divided into spherical sectors (in red), double-cone cells (in yellow) and tetrahedrons (in blue), respectively corresponding to the 2-patches, 1-patches (circular arcs) and 0-patches (intersection points) on Γ.

In summary, the group of subregions $\{\mathcal{R}(\gamma_i^{(k)})\}$ with $0 \le k \le d-1$ and $1 \le i \le n_k$ provide a partition of $\overline{\Omega}$. In fact, for any point $\mathbf{p} \in \overline{\Omega}$, we have $\mathbf{p} \in \mathcal{R}(\gamma_i^{(k)})$ if and only if $\mathbf{p}$ has a closest point in $\gamma_i^{(k)}$. Therefore, this newly-proposed diagram allows to find efficiently a closest point on Γ to $\mathbf{p}$ and consequently, to compute the signed distance $f_\Gamma(\mathbf{p})$. We mention that the volume (resp. area) of the union of balls (resp. discs) can be computed based on the Voronoi-type diagram, which will be presented in Section 3.

3. Application I: volume of the union of d-balls. The Voronoi-type diagram can be used to calculate the volume of Ω, given all components of Γ.

3.1. General formula. Consider an arbitrary k-patch $\gamma_i^{(k)}$ on Γ, $1 \le k \le d-1$, $1 \le i \le n_k$. We suppose that $\gamma_i^{(k)}$ is part of a k-sphere with center $\mathbf{c}_i^{(k)}$ and radius

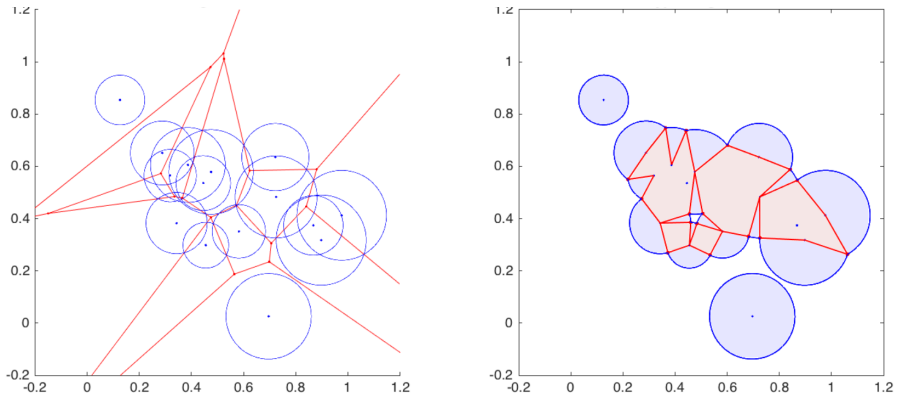

FIG. 3. *The power diagram (left) and the Voronoi-type diagram (right) of a same group of circles in* $\mathbb{E}^2$.

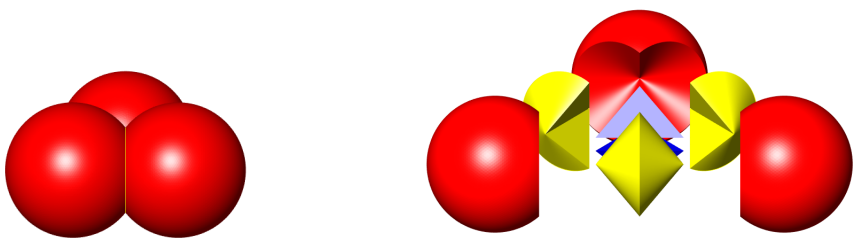

FIG. 4. *The union of three intersected* 3*-balls (left) and its Voronoi-type diagram (right).*

$r_i^{(k)}$. According to Eq. (2.27), we can compute

(3.1)
$$\begin{aligned}\mathcal{R}(\gamma_i^{(k)}) &= \bigcup_{\mathbf{x}\in\gamma_i^{(k)}} \operatorname{conv}(\mathbf{x},\mathbf{c_i}) \\ &= \left\{\mathbf{y} \mid \mathbf{y} = \lambda\mathbf{x} + \sum_{t=1}^{m}\lambda_t\mathbf{c}_{i_t},\ \mathbf{x}\in\gamma_i^{(k)},\ \lambda + \sum_{t=1}^{m}\lambda_t = 1,\ 0\le\lambda,\lambda_t\le 1\right\} \\ &= \left\{\mathbf{y} \mid \mathbf{y} = \lambda\mathbf{x} + (1-\lambda)\mathbf{z},\ \mathbf{x}\in\gamma_i^{(k)},\ \mathbf{z}\in\operatorname{conv}(\mathbf{c_i}),\ 0\le\lambda\le 1\right\},\end{aligned}$$

where $\mathbf{i} = \mathcal{I}(\gamma_i^{(k)}) = \{i_1, i_2, \ldots, i_m\}$. Then, we propose the following lemma on calculating the d-dimensional volume (d-volume) of the cell $\mathcal{R}(\gamma_i^{(k)})$ when $k \ge 1$.

LEMMA 3.1. *The* d*-volume of* $\mathcal{R}(\gamma_i^{(k)})$ *can be characterized as follows*

$$\operatorname{Vol}^{(d)}\left(\mathcal{R}(\gamma_i^{(k)})\right) = r_i^{(k)}\,\mathrm{B}(k+1, d-k)\,\operatorname{Vol}^{(k)}\left(\gamma_i^{(k)}\right)\operatorname{Vol}^{(d-k)}\left(\operatorname{conv}(\mathbf{c_i})\right), \tag{3.2}$$

where $\operatorname{Vol}^{(k)}(\gamma)$ *denotes the* k*-volume of a* k*-dimensional surface* γ*,* $r_i^{(k)}$ *denotes the radius of the* k*-sphere containing* $\gamma_i^{(k)}$ *and* $\mathrm{B}(\cdot,\cdot)$ *is the Beta function.*

Proof. We define two sets $\Sigma \coloneqq \gamma_i^{(k)} - \mathbf{c}_i^{(k)}$ and $\Pi \coloneqq \mathrm{conv}\,(\mathbf{c_i}) - \mathbf{c}_i^{(k)}$, where $\mathbf{c}_i^{(k)}$ is the center of the k-sphere containing $\gamma_i^{(k)}$. From Lemma 2.2, we then conclude that $\Sigma \perp \Pi$. Further, Σ and Π are respectively of dimension k and $d-k-1$. According to Eq. (3.1), we can write $\mathcal{R}(\gamma_i^{(k)})$ as follows

$$\mathcal{R}(\gamma_i^{(k)}) = \left\{ \mathbf{y} \mid \mathbf{y} = \mathbf{c}_i^{(k)} + \frac{r}{r_i^{(k)}}\sigma + \left(1 - \frac{r}{r_i^{(k)}}\right)\tau,\ \sigma \in \Sigma,\ \tau \in \Pi,\ 0 \le r \le r_i^{(k)} \right\}. \tag{3.3}$$

Since $\Sigma \perp \Pi$, the volume infinitesimal $\mathrm{d}\mathbf{y}$ can be written as

$$\mathrm{d}\mathbf{y} = \left(\frac{r}{r_i^{(k)}}\right)^k \left(1 - \frac{r}{r_i^{(k)}}\right)^{d-k-1} \mathrm{d}r\mathrm{d}\sigma\mathrm{d}\tau.$$

We can consequently compute

$$\begin{aligned} &\mathrm{Vol}^{(d)}\left(\mathcal{R}(\gamma_i^{(k)})\right) \\ &= \int_0^{r_i^{(k)}} \left(\frac{r}{r_i^{(k)}}\right)^k \left(1 - \frac{r}{r_i^{(k)}}\right)^{d-k-1} \mathrm{d}r \int_\Sigma \mathrm{d}\sigma \int_\Pi \mathrm{d}\tau \\ &= r_i^{(k)} \left(\int_0^1 \lambda^k (1-\lambda)^{d-k-1} \mathrm{d}\lambda\right) \mathrm{Vol}^{(k)}\left(\gamma_i^{(k)}\right) \mathrm{Vol}^{(d-k-1)}\left(\mathrm{conv}(\mathbf{c_i})\right) \\ &= r_i^{(k)}\, \mathrm{B}(k+1, d-k)\, \mathrm{Vol}^{(k)}\left(\gamma_i^{(k)}\right) \mathrm{Vol}^{(d-k-1)}\left(\mathrm{conv}\,(\mathbf{c_i})\right). \end{aligned} \tag{3.4}$$

where $\mathrm{B}(\cdot,\cdot)$ is the Beta function [15]. □

We now consider an abitrary intersection point $\gamma_i^{(0)}$ with $0 \le i \le n_0$. Suppose that $\gamma_i^{(0)}$ is an endpoint of some 1-patches denoted by $\{\gamma_{ij}^{(1)}\}_{j=1,\dots,K_i}$. Recall that $\Lambda_{\mathcal{I}(\gamma_i^{(0)})}$ denotes the affine space defined in (2.7) . In the degenerate case, $\gamma_i^{(0)}$ lies in the affine space $\Lambda_{\mathcal{I}(\gamma_i^{(0)})}$ which is in this case of dimension

$$\dim\left(\Lambda_{\mathcal{I}(\gamma_i^{(0)})}\right) \le d-1, \tag{3.5}$$

as presented in the proof of Lemma 2.2. In this case, $\gamma_i^{(0)}$ is actually generated by a $(d-1)$-sphere and a tangent affine space. According to Theorem 2.5, we have $\mathcal{R}(\gamma_i^{(0)}) \subseteq \Lambda_{\mathcal{I}(\gamma_i^{(0)})}$ and therefore,

$$\dim\left(\mathcal{R}(\gamma_i^{(0)})\right) \le d-1. \tag{3.6}$$

As a consequence, the volume of the Voronoi-type cell corresponding to a degenerate intersection point is

$$\mathrm{Vol}^{(d)}\left(\mathcal{R}(\gamma_i^{(0)})\right) = 0. \tag{3.7}$$

This implies that the degenerate intersection points can be ignored in the computation of $\mathrm{Vol}^{(d)}(R_0)$. In the nondegenerate case, $\gamma_i^{(0)}$ is generated by the intersection of a $(d-1)$-sphere and some line passing through the sphere. In this case, there do exist

some 1-patches (circular arcs) having $\gamma_i^{(0)}$ as an endpoint, implying that $K_i > 0$. Further, it holds that

$$\dim\left(\Lambda_{\mathcal{I}(\gamma_{ij}^{(1)})}\right) = d-2, \qquad \forall j = 1, 2, \ldots, K_i, \tag{3.8}$$

according to Lemma 2.2. Then, we can denote the $(d-1)$-dimensional face corresponding to $\gamma_{ij}^{(1)}$ by

$$F_{ij} \coloneqq \operatorname{conv}\left(\gamma_i^{(0)}, \mathbf{c}_{\mathcal{I}(\gamma_{ij}^{(1)})}\right), \tag{3.9}$$

where $\mathbf{c}_{\mathcal{I}(\gamma_{ij}^{(1)})}$ is a set of spherical centers given by (2.6) and F_{ij} is actually a tetrahedron in some $(d-1)$-hyperplane. We define the set of all nondegenerate intersection points as $\widetilde{P}_0$. Then, we propose the following lemma for computing $\mathrm{Vol}^{(d)}(R_0)$ where R_0 is defined in (2.29).

Lemma 3.2. *The volume of R_0 can be computed as*

$$\mathrm{Vol}^{(d)}(R_0) = \sum_{i=1}^{n_0}\sum_{j=1}^{K_i} \frac{1}{d}\left(\mathbf{n}_{ij}\cdot\gamma_i^{(0)}\right)\mathrm{Vol}^{(d-1)}(F_{ij}), \tag{3.10}$$

where $\mathbf{n}_{ij}$ denotes the outward-pointing normal vector of F_{ij}. We make a convention that $\mathbf{n}_{ij} = \mathbf{0}$ when $\gamma_i^{(0)}$ is a degenerate intersection point.

Proof. Denote by $\widetilde{R}_0$ the union of all Voronoi-type cells associated with nondegenerate intersection points in $\widetilde{P}_0$, that is,

$$\widetilde{R}_0 = \mathcal{R}\left(\widetilde{P}_0\right). \tag{3.11}$$

According to the definition (2.29) of R_0 and Eq. (3.7), we know that

$$\mathrm{Vol}^{(d)}(R_0) = \mathrm{Vol}^{(d)}\left(\widetilde{R}_0\right). \tag{3.12}$$

Claim 3.3. *The boundary of $\widetilde{R}_0$ can be characterized as*

$$\partial\widetilde{R}_0 = \bigcup_{\substack{1\le i\le n_0\\ 1\le j\le K_i}} F_{ij} \bigcup F_0, \tag{3.13}$$

where F_0 is some subset on $\partial\widetilde{R}_0$ with $\dim(F_0) \le d-2$.

The proof of Claim 3.3 is presented in Appendix B. According to the Gauss-Green theorem, we can further compute

$$\begin{aligned}
\mathrm{Vol}^{(d)}(\widetilde{R}_0) &= \int_{\widetilde{R}_0} \frac{1}{d}\left(\nabla\cdot\mathbf{y}\right)\mathrm{d}\mathbf{y}\\
&= \frac{1}{d}\int_{\partial\widetilde{R}_0}\left(\mathbf{n}\cdot\mathbf{y}\right)\mathrm{d}\sigma_{\mathbf{y}}\\
&= \sum_{i=1}^{n_0}\sum_{j=1}^{K_i}\frac{1}{d}\int_{F_{ij}}\left(\mathbf{n}_{ij}\cdot\mathbf{y}\right)\mathrm{d}\sigma_{\mathbf{y}}\\
&= \sum_{i=1}^{n_0}\sum_{j=1}^{K_i}\frac{1}{d}\left(\mathbf{n}_{ij}\cdot\gamma_i^{(0)}\right)\mathrm{Vol}^{(d-1)}(F_{ij}),
\end{aligned} \tag{3.14}$$

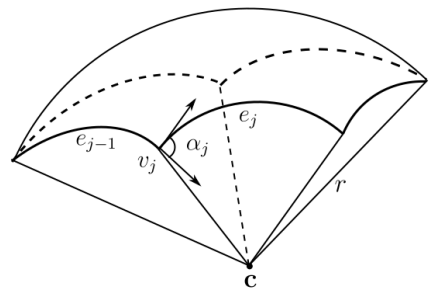

FIG. 5. *Schematic diagram of notations associated with a spherical patch γ with center $\mathbf{c}$ and radius r. α_j is the angle variation between two neighboring circular arcs e_{j-1} and e_j at the vertex v_j of γ.*

where $\mathrm{d}\sigma_{\mathbf{y}}$ denotes the surface measure. In the last equality, we use the fact that F_{ij} lies in a hyperplane and $\mathbf{n}_{ij} \cdot \mathbf{y}$ is constant. ∎

In summary, given the components of its boundary Γ, we obtain an explicit expression of the volume of the union of balls Ω according to Lemma 3.1 and 3.2 as follows

$$\begin{aligned}\mathrm{Vol}^{(d)}(\Omega) = &\sum_{k=1}^{d-1}\sum_{i=1}^{n_k} r_i^{(k)}\,\mathrm{B}(k+1, d-k)\,\mathrm{Vol}^k\left(\gamma_i^{(k)}\right)\,\mathrm{Vol}^{d-k}\left(\mathrm{conv}\left(\mathbf{c_i}\right)\right)\\ &+\sum_{i=1}^{n_0}\sum_{j=1}^{K_i}\frac{1}{d}\left(\mathbf{n}_{ij}\cdot\gamma_i^{(0)}\right)\mathrm{Vol}^{(d-1)}\left(F_{ij}\right).\end{aligned} \tag{3.15}$$

Remark 3.4. In $\mathbb{E}^3$, the volume formula (3.15) is more convenient to implement than the power diagram, because one no more needs to compute the boundary polygons of the power cells, which can be very technical [7].

3.2. Analytical volume in 3D. We have given an explicit formula of the volume of Ω, which is based on the Voronoi-type diagram. In the cases of $\mathbb{E}^2$ and $\mathbb{E}^3$, the different components of Γ are not difficult to compute. In this subsection, we consider the case of $\mathbb{E}^3$ as an illustration.

The boundary of the union of 3-balls is constituted by the intersection points, the circular arcs (or circles) and the spherical 2-patches. The length of a circular arc is easy to compute and the area of a spherical 2-patch can be computed by the Gauss-Bonnet theorem [8]. For the sake of completeness, we present here the explicit formula of the area of a spherical 2-patch γ with the notations in Figure 5 as follows (see [16] for details)

$$\sum_j \alpha_j + \sum_j k_{e_j}|e_j| + \frac{1}{r^2}\,\mathrm{Area}\,(\gamma) = 2\pi\chi, \tag{3.16}$$

where α_j is the angle at vertex v_i between two neighboring circular arcs e_{j-1} and e_j, k_{e_j} is the geodesic curvature of e_j, $|e_j|$ is the length of e_j, $\mathrm{Area}\,(\gamma)$ is the area of γ. In addition, χ is the Euler characteristic of γ, which equals to 2 minus the number of loops forming the boundary of γ.

From the volume formulation (3.15) in the previous subsection, we obtain the

TABLE 1

Volumes of the union of SAS-balls for different molecules. The VDW radii and atomic centers are derived from the protein data bank [5]. The solvent probe's radius is set to 1. *N represents the number of SAS-balls and* Vol *represents the volume.*

	Caffeine	1YJO	1ETN	1B17	101M	2K4C
N	24	67	160	483	1413	2443
Vol	5.0327e+02	2.1100e+03	2.9076e+03	1.2786e+04	3.3379e+04	3.8126e+04

volume of the union (still denoted by $\overline{\Omega}$) of balls in $\mathbb{E}^3$:

$$\begin{aligned}\mathrm{Vol}^{(3)}(\Omega) = \frac{1}{3}\sum_{i=1}^{n_2} r_i^{(2)}\,\mathrm{Area}(\gamma_i^{(2)}) + \frac{1}{6}\sum_{i=1}^{n_1} r_i^{(1)}\,d_i^{(1)}\,\left|\gamma_i^{(1)}\right| \\ + \frac{1}{3}\sum_{i=1}^{n_0}\sum_{j=1}^{K_i}\left(\mathbf{n}_{ij}\cdot\gamma_i^{(0)}\right)\,\mathrm{Area}\left(F_{ij}\right),\end{aligned} \tag{3.17}$$

where $r_i^{(2)}$ denotes the radius of the 2-patch $\gamma_i^{(2)}$, $r_i^{(1)}$ denotes the radius of the circular arc $\gamma_i^{(1)}$, $d_i^{(1)}$ denotes the distance between the centers of the two spheres generating $\gamma_i^{(1)}$.

EXAMPLE 3.5. *In Table 1, we compute the volumes of different solvent excluded surface (SAS) cavities [16] constituted by SAS-balls in $\mathbb{E}^3$. Each SAS-ball is centered at the corresponding atomic center and has a radius equal to the sum of the van der Waals (VDW) radius and the solvent probe's radius.*

In a high-dimensional space $\mathbb{E}^d$ with $d > 3$, it is difficult or costly to compute the surface volumes of the boundary components of Γ. As a consequence, it is not easy to compute the analytical volume based on the use of the Voronoi-type diagram, unless the boundary components are known. In the power diagram, the same difficulty also exists. In Appendix C, we present how the Voronoi-type diagram can be used to compute approximately the volume for a simple example in hight dimension. Next, let us consider another application of the Voronoi-type diagram to characterize a molecular surface.

4. Application II: characterization of the SES. For the sake of completeness, we introduce briefly how the Voronoi-type diagram can be used in the characterization of the "smooth" molecular surface in $\mathbb{E}^3$, which has been presented in the previous work [16] of some of us.

In the implicit solvation models in quantum chemistry, the solute molecule is commonly regarded as a union of atomic balls, such as the van der Waals balls. Meanwhile, the solvent molecule can be simply idealized as a spherical probe. As introduced in Example 3.5, the SAS denoted by Γ_{sas} is the boundary of the union of the SAS-balls whose radii are equal to the sum of the VDW radii $\{r_i\}_{i=1}^N$ and the fixed probe's radius r_{p}. Denote the signed distance function to the SAS by f_{sas} in the form of (2.2). The solvent excluded surface (SES, denoted by Γ_{ses}) is defined as the level set of f_{sas} as follows

$$\Gamma_{\mathrm{ses}} := f_{\mathrm{sas}}^{-1}(-r_{\mathrm{p}}), \tag{4.1}$$

which is a well-known concept in the chemistry community and is also called the "smooth" molecular surface. For a better visual understanding, Figure 6 illustrates

the SES of the molecule 1B17. It is observed that the SES is composed of three types of patches: convex spherical patches (in red), toroidal patches (in yellow) and concave spherical patches (in blue). These patches corresponds respectively to the 2-patches, the 1-patches (circular arcs in yellow) and the 0-patches (intersection points in blue) on Γ_{sas}.

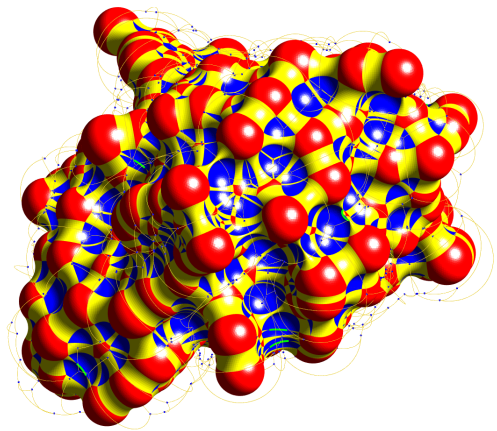

FIG. 6. *The SES of the molecule 1B17 with the solvent probe's radius* $r_{\text{p}} = 1.5$. *The green arcs are SES-singularities.*

The Voronoi-type diagram gives a partition of the SAS-cavity, i.e., a set of non-overlapping cells. For a given point in the SAS-cavity, one can obtain its closest point to Γ_{sas} by determining which cell this point lies in. This means that the signed distance f_{sas} is computable. Further, with the same notations as introduced previously, the SES-patch $\mathcal{P}_i^{(k)}$ corresponding to the spherical patch $\gamma_i^{(k)}$ on Γ_{sas} can be written mathematically as

$$\mathcal{P}_i^{(k)} = \mathcal{R}(\gamma_i^{(k)}) \cap f_{\text{sas}}^{-1}(-r_{\text{p}}) = \mathcal{R}(\gamma_i^{(k)}) \cap f_{\gamma_i^{(k)}}^{-1}(-r_{\text{p}}), \qquad \forall k = 0, 1, 2. \tag{4.2}$$

where $f_{\gamma_i^{(k)}}$ denotes the signed distance function to $\gamma_i^{(k)}$ in the cell $\mathcal{R}(\gamma_i^{(k)})$. In summary, the SES can be completely characterized based on the Voronoi-type diagram (see more details in [16]).

Remark 4.1. Generally speaking, given an arbitrary surface in 3D, the signed distance from a point to this surface is difficult (or expensive) to compute analytically. However, in the case of the boundary of the union of balls, the Voronoi-type diagram allows to compute this value directly.

Remark 4.2. Any point $\mathbf{x} \in \mathbb{R}^3$ is singular (in the sense that f_{sas} is nondifferentiable at $\mathbf{x}$) if and only if it has more than one closest points on Γ_{sas}. The Voronoi-type diagram allows us to count the number of closest points for any point $\mathbf{x}$. Therefore, the singularities on the SES can be computed a priori, see [16]. This concept is generally known as medial axis which is discussed in the next section.

5. Application III: medial axis. The medial axis of an object is the set of all points having more than one closest points on the object's boundary. This concept was first introduced by Blum [6] and was originally referred to as the topological skeleton. It has been showed that the medial axis of an object is always homotopy

equivalent to the object itself [12]. Therefore, the medial axis is useful for shape description. The problem is that computing the medial axis of a general object can be difficult. Usually, the object is first approximated by a finite union of balls and then the medial axis of this union of balls can be computed [2, 1, 10].

Based on the proposed Voronoi-type diagram of the union of d-balls, we study the medial axis of a union of d-balls in different cells. We first consider the medial axis in the Voronoi-type cell $\mathcal{R}(\gamma_i^{(k)})$, for a spherical k-patch $\gamma_i^{(k)}$ with $1 \le k \le d-1$. According to Corollary 2.7, we can claim that $\mathrm{conv}(\mathbf{c_i})$ is part of the medial axis where $\mathbf{i} = \mathcal{I}(\gamma_i^{(k)})$. The reason is that $\forall \mathbf{x} \in \mathrm{conv}(\mathbf{c_i})$, any point on $\gamma_i^{(k)}$ is a closest point of $\mathbf{x}$. Then, we consider the medial axis in R_0. For an arbitrary intersection point $\gamma_i^{(0)}$, we know that the set $\partial\mathcal{R}(\gamma_i^{(0)}) \cap \mathrm{Vor}(\gamma_i^{(0)})$ is part of the medial axis (see Section 2.3), where each point has at least two intersection points as its closest points.

Here, we illustrate a simple example of the medial axis of caffeine molecule in Figure 7.

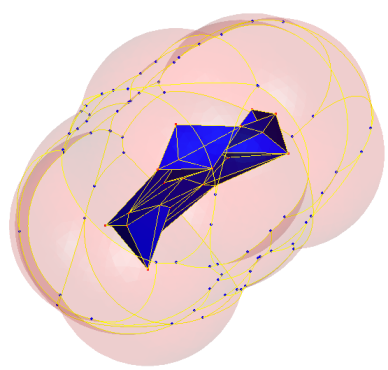

FIG. 7. *Medial axis of caffeine molecule, composed of red points, yellow line segments and blue faces, respectively in different Voronoi-type cells.*

6. Conclusion. In this article, we have proposed a Voronoi-type diagram of the union of d-balls, which can be seen as an alternative to the well-known power diagram. We have introduced some properties of this new diagram, as well as its applications in the volume computation, the characterization of molecular surfaces and the medial axis of a union of balls. At this moment, the applications of this diagram are restricted to $\mathbb{E}^2$ and $\mathbb{E}^3$. We expect more possible applications in the high dimensional spaces in the future.

Appendix A. Proof of Claim 2.6. First, we consider a sphere $S_{i_t} \ni \mathbf{x}$ for a fixed $1 \le t \le m$. According to the definition (2.19) and Eq. (2.21), we can compute

$$\begin{aligned}
&|\zeta_s(x) - \mathbf{c}_{i_t}|^2 - |\mathbf{x} - \mathbf{c}_{i_t}|^2 \\
&= |x\mathbf{n}_s + \alpha(x)\mathbf{v}|^2 - 2\,(\mathbf{v}_t, x\mathbf{n}_s + \alpha(x)\mathbf{v}) \\
&= \left(\alpha^2(x)|\mathbf{v}|^2 + x^2\right) + 2x\alpha(x)\,(\mathbf{n}_s, \mathbf{v}) - 2\alpha(x)(\mathbf{v}, \mathbf{v}_t) - 2x(\mathbf{v}_t, \mathbf{n}_s) \\
&= 2\alpha(x)(\mathbf{v}, \mathbf{v} - \mathbf{v}_t) - 2x(\mathbf{v}_t, \mathbf{n}_s) \\
&= 2x\left[-(\mathbf{v}_t, \mathbf{n}_s) + \frac{x}{|\mathbf{v}|^2(2-\alpha(x))}(\mathbf{v}, \mathbf{v} - \mathbf{v}_t)\right],
\end{aligned} \tag{A.1}$$

where in the third and forth equality, we use the fact that $\alpha^2(x)|\mathbf{v}|^2 + x^2 = 2\alpha(x)|\mathbf{v}|^2$ and $(\mathbf{n}_s, \mathbf{v}) = 0$ as $\mathbf{v}_r \in \mathcal{A}_s$.

Since $(\mathbf{x}+\lambda\mathbf{v}_t,\mathbf{n}_s)\le b_s,\ \forall\lambda\ge 0$, we know that $(\mathbf{v}_t,\mathbf{n}_s)\le 0$. In the case of $(\mathbf{v}_t,\mathbf{n}_s)<0$, according to Eq. (A.1), there exists a small enough number $\varepsilon_{i_t}>0$ such that $\forall x\in[0,\varepsilon_{i_t}]$,

$$|\zeta_s(x)-\mathbf{c}_{i_t}|\ge|\mathbf{x}-\mathbf{c}_{i_t}|=r_{i_t}.$$

Besides, in the case of $(\mathbf{v}_t,\mathbf{n}_s)=0$ implying $\mathbf{v}_t\in\mathcal{A}_s$, according to Eq. (2.23) and (A.1), we have $\forall 0\le x\le|\mathbf{v}|$,

$$|\zeta_s(x)-\mathbf{c}_{i_t}|\ge|\mathbf{x}-\mathbf{c}_{i_t}|=r_{i_t}.$$

In particular, when $t=t_0$, we have both $(\mathbf{v}_t,\mathbf{n}_s)=0$ and $(\mathbf{v},\mathbf{v}-\mathbf{v}_t)=0$. As a consequence,

$$|\zeta_s(x)-\mathbf{c}_{i_t}|=|\mathbf{x}-\mathbf{c}_{i_t}|=r_{i_t},$$

which means that $\zeta_s(x)\in S_{i_{t_0}}$. So far, we have proved that $\forall x\in[0,\varepsilon_{i_t}]$, $\zeta_s(x)$ does not lie in the interior of S_{i_t} and lies on the sphere $S_{i_{t_0}}$.

Second, we consider a sphere $S_j\notin\{S_{i_1},S_{i_2},\dots,S_{i_m}\}$ that does not contain $\mathbf{x}$. In this case, we have $|\mathbf{x}-\mathbf{c}_j|-r_j>0$. Therefore, there exists a small number $\varepsilon_j>0$ such that $\forall x\in[0,\varepsilon_j]$,

$$|\zeta_s(x)-\mathbf{x}|\le\frac{1}{2}(|\mathbf{x}-\mathbf{c}_j|-r_j).$$

This yields that $\forall x\in[0,\varepsilon_j]$,

$$|\zeta_s(x)-\mathbf{c}_j|\ge|\mathbf{x}-\mathbf{c}_j|-|\zeta_s(x)-\mathbf{x}|\ge\frac{1}{2}(|\mathbf{x}-\mathbf{c}_j|+r_j)>r_j,$$

that is to say, $\zeta_s(x)$ lies outside the sphere S_j.

In summary, there exists a possibly small number $\varepsilon>0$ such that $\forall x\in[0,\varepsilon]$, $\zeta_s(x)$ does not cross any sphere S_i and lies on the sphere $S_{i_{t_0}}$, which implies that $\zeta_s(x)\in\Gamma$.

Appendix B. Proof of Claim 3.3 . Recall the definition of the face

$$F_{ij}:=\operatorname{conv}\left(\gamma_i^{(0)},\mathbf{c}_{\mathcal{I}(\gamma_{ij}^{(1)})}\right),\qquad 1\le i\le n_0,\ 1\le j\le K_i. \tag{B.1}$$

Given a nondegenerate intersection point $\gamma_i^{(0)}$ and the associated 1-patch $\gamma_{ij}^{(1)}$, the $(d-1)$-face F_{ij} is actually a subset of $\widetilde{R}_0$, since, according to Lemma 2.4, F_{ij} is a subset of $\mathcal{R}(\gamma_i^{(0)})$. Further, taking any point $\mathbf{y}\in\gamma_{ij}^{(1)}$, we have the following result

$$\mathcal{R}(\mathbf{y})=\operatorname{conv}\left(\mathbf{y},\mathbf{c}_{\mathcal{I}(\gamma_{ij}^{(1)})}\right)\subseteq\mathcal{R}\left(\gamma_{ij}^{(1)}\right). \tag{B.2}$$

As $\mathbf{y}$ tends to $\gamma_i^{(0)}$, $\mathcal{R}(\mathbf{y})$ tends to F_{ij}. Any interior point of $\mathcal{R}(\mathbf{y})$ has $\mathbf{y}$ as a unique closest point, which implies that the interior of $\mathcal{R}(\mathbf{y})$ lies completely outside $\widetilde{R}_0$. For any point $\mathbf{x}\in F_{ij}$, we can then find a sequence of points $\{\mathbf{x}_n\}$ outside $\widetilde{R}_0$ converging to $\mathbf{x}$. Therefore, we have $F_{ij}\subseteq\partial\widetilde{R}_0$.

It is sufficient to prove that any point $\mathbf{x}\in\partial\widetilde{R}_0$ belongs to either some face F_{ij} or some set F_0 with $\dim(F_0)\le d-2$. $\partial\widetilde{R}_0$ can be divided into two sets

$$U_1:=\{\mathbf{x}\in\partial\widetilde{R}_0\mid\ \text{all closest points of }\mathbf{x}\text{ belong to }\widetilde{P}_0\}, \tag{B.3}$$

and

$$U_2 \coloneqq \{\mathbf{x} \in \partial \widetilde{R}_0 \mid \text{ there exists a closest point of } \mathbf{x} \text{ not contained in } \widetilde{P}_0\}. \tag{B.4}$$

In the following content, we prove that if $\mathbf{x} \in U_1$, then $\mathbf{x}$ belongs to a certain face F_{ij}, while if $\mathbf{x} \in U_2$, then $\mathbf{x}$ belongs to F_0 which will be defined later.

Step 1: In the case of $\mathbf{x} \in U_1$, we can find a sequence of points $\{\mathbf{x}_n\}$ in $\Omega \backslash R_0$ such that $\mathbf{x}_n$ tends to $\mathbf{x}$. Correspondingly, there exists a sequence of points $\{\mathbf{a}_n\}$ on Γ, where $\mathbf{a}_n$ is one closest point of $\mathbf{x}_n$. Since $\mathbf{x}$ has finitely many closest points in $\widetilde{P}_0$ and the total number of k-patches is finite, we can extract a subsequence of $\mathbf{a}_n$ such that this subsequence lies on some k-patch $\gamma^{(k)}$ with $k \geq 1$ and converges to some nondegenerate intersection point $\gamma_i^{(0)}$. Without loss of generality, we can therefore suppose that $\mathbf{a}_n$ tends to $\gamma_i^{(0)}$ and $\mathbf{a}_n \in \gamma^{(k)}$, $\forall n$. As a consequence, $\gamma_i^{(0)}$ is on the boundary of $\gamma^{(k)}$ and further, there exists a 1-patch $\gamma_{ij}^{(1)}$ on $\overline{\gamma}^{(k)}$, satisfying

$$\mathbf{c}_{\mathcal{I}(\gamma^{(k)})} \subseteq \mathbf{c}_{\mathcal{I}(\gamma_{ij}^{(1)})}. \tag{B.5}$$

Due to the fact that

$$\mathbf{x}_n \in \operatorname{conv}\left(\mathbf{a}_n, \mathbf{c}_{\mathcal{I}(\gamma^{(k)})}\right), \tag{B.6}$$

we then have

$$\mathbf{x} \in \operatorname{conv}\left(\gamma_i^{(0)}, \mathbf{c}_{\mathcal{I}(\gamma^{(k)})}\right) \subseteq \operatorname{conv}\left(\gamma_i^{(0)}, \mathbf{c}_{\mathcal{I}(\gamma_{ij}^{(1)})}\right) = F_{ij}, \tag{B.7}$$

by taking $n \to \infty$.

Step 2: In the case of $\mathbf{x} \in U_2$, we want to prove that $\mathbf{x}$ belongs to some F_0. According to the definition of U_2, $\mathbf{x}$ has at least one closest point $\mathbf{a}$ that is not a nondegenerate intersection point. Here, we mention the fact that for any point $\mathbf{y}$ belonging to the open line segment $\overline{\mathbf{ax}}$ with endpoints $\mathbf{a}$ and $\mathbf{x}$, $\mathbf{a}$ is the unique closest point of $\mathbf{y}$ on Γ, which can be easily proven by contradiction.

On the one hand, if $\mathbf{a}$ is not an intersection point, then $\mathbf{a}$ lies on some k-patch $\gamma^{(k)}$ with $k \geq 1$. According to Theorem 2.5, we know that

$$\mathcal{R}(\mathbf{a}) = \operatorname{conv}\left(\mathbf{a}, \mathbf{c}_{\mathcal{I}(\gamma^{(k)})}\right). \tag{B.8}$$

Considering that the latter convex hull, we obtain that $\mathbf{x} \in \operatorname{conv}(\mathbf{c}_{\mathcal{I}(\gamma^{(k)})})$ of dimension $\dim(\operatorname{conv}(\mathbf{c}_{\mathcal{I}(\gamma^{(k)})})) \leq d-2$, since otherwise, $\mathbf{x}$ will has a unique closest point on Γ. On the other hand, if $\mathbf{a}$ is a degenerate intersection point, then we have $\mathbf{a} \in \Lambda_{\mathcal{I}(\mathbf{a})}$ with $\dim\left(\Lambda_{\mathcal{I}(\mathbf{a})}\right) \leq d-1$. Since $\mathcal{R}(\mathbf{a}) \subseteq \Lambda_{\mathcal{I}(\mathbf{a})}$ according to Theorem 2.5, it holds that $\dim\left(\mathcal{R}(\mathbf{a})\right) \leq d-1$. Here, we actually have $\mathbf{a} \in \mathcal{R}(\mathbf{a})$ and $\mathcal{R}(\mathbf{a})$ is a convex set from Lemma 2.4. Due to the fact mentioned above, we obtain that $\mathbf{x} \in \mathcal{R}(\mathbf{a})$ only lies on $\partial\mathcal{R}(\mathbf{a})$ of dimension $\dim\left(\partial\mathcal{R}(\mathbf{a})\right) \leq d-2$.

As the number of k-patches and degenerate intersection points are finite, we can conclude that

$$\mathbf{x} \in \bigcup_{k \geq 1} \operatorname{conv}(\mathbf{c}_{\mathcal{I}(\gamma^{(k)})}) \bigcup_{\gamma_i^{(0)} \notin \widetilde{P}_0} \partial\mathcal{R}(\gamma_i^{(0)}), \qquad \forall \mathbf{x} \in U_2, \tag{B.9}$$

where $\gamma_i^{(0)}$ in the second union is taken as all degenerate intersection points. Note that the union on the right-hand side of Eq. (B.9) is of dimension less than or equal

TABLE 2
Centers and radii of 2-spheres.

	$S_{12}^{(2)}$	$S_{13}^{(2)}$	$S_{14}^{(2)}$	$S_{23}^{(2)}$	$S_{24}^{(2)}$	$S_{34}^{(2)}$
center	$(0,\frac{1}{2},0,0)$	$(\frac{1}{2},0,0,0)$	$(\frac{1}{2},\frac{1}{2},0,0)$	$(\frac{1}{2},\frac{1}{2},0,0)$	$(\frac{1}{2},1,0,0)$	$(1,\frac{1}{2},0,0)$
radius	$\sqrt{\frac{3}{4}}$	$\sqrt{\frac{3}{4}}$	$\sqrt{\frac{1}{2}}$	$\sqrt{\frac{1}{2}}$	$\sqrt{\frac{3}{4}}$	$\sqrt{\frac{3}{4}}$
N_{ext}	788730	788730	0	0	788494	788494

to $d-2$. This implies that $\dim(U_2) \leq d-2$. Therefore, we can define $F_0 = U_2$, which satisfies $\dim(F_0) \leq d-2$.

Appendix C. Approximate volume in high-dimensional spaces. In the high-dimensional space $\mathbb{E}^d$ with $d > 3$, one can also compute the approximate volume of the union of d-balls based on Eq. (3.15). As mentioned above, the k-volume of a spherical k-patch $\gamma_i^{(k)}$ on Γ can be difficult to compute analytically. Therefore, we consider to use the Monte Carlo method to approximate the volume.

We first take a k-sphere denoted by $S^{(k)}$, which is formed by the intersection of some $(d-1)$-spheres (or only one sphere in the case of $k = d-1$). Then, we generate a set of uniformly distributed random points on this k-sphere, using the method in [13]. Suppose that the total number of the random points is N_{tot} and there are N_{ext} exterior points that are not covered by any d-ball. The k-volume of all k-patches lying on $S^{(k)}$ can be approximated as follows

$$\text{Vol}_{\text{ext}} \approx \frac{N_{\text{ext}}}{N_{\text{tot}}} \text{Vol}^{(k)}(S^{(k)}), \tag{C.1}$$

which is actually the volume of the exterior part of $S^{(k)}$. With the approximate volume Vol_{ext} for each k-sphere, we can consequently compute $\text{Vol}\,(\Omega)$ according to Eq. (3.15). Here is a simple example in the case of four spheres in $\mathbb{E}^4$.

EXAMPLE C.1. *Take four 4-balls $\{B_1, B_2, B_3, B_4\}$ in $\mathbb{E}^4$ with the same radius 1 and the centers $(0,0,0,0)$, $(0,1,0,0)$, $(1,0,0,0)$ and $(1,1,0,0)$. Compute the approximate volume of the union of these 4-balls.*

First, there are four 3-spheres $\{S_1^{(3)}, S_2^{(3)}, S_3^{(3)}, S_4^{(3)}\}$ corresponding to the four 4-balls. We take a set of 10^6 uniformly distributed random points on the unit 3-sphere, denoted by P. For each 3-sphere with center $\mathbf{c}$, we test: $\forall \mathbf{s} \in P$, whether $\mathbf{c}+\mathbf{s}$ is covered by any other balls or not. We use the Monte Carlo method and count the number of exterior points for each 3-sphere: 634184, 633896, 634385 and 633850. As a consequence, according to Eq. (C.1), we can compute approximately

$$\text{Vol}^{(3)}\left(\bigcup_i \gamma_i^{(3)}\right) \approx \frac{634184 + 633896 + 634385 + 633850}{10^6} \times 2\pi^2. \tag{C.2}$$

Second, there are six 2-spheres $\{S_{12}^{(2)}, S_{13}^{(2)}, S_{14}^{(2)}, S_{23}^{(2)}, S_{24}^{(2)}, S_{34}^{(2)}\}$, which are generated by the intersection of six pairs of 3-spheres. Then, we take 10^6 random points on the unit 2-sphere and use the Monte Carlo method to approximate the area of the exterior part of each 2-sphere. Here is the table of the centers, the radii and the number of the exterior points on the 2-spheres.

Again, according to Eq. (C.1), we can compute approximately

$$\mathrm{Vol}^{(2)}\left(\bigcup_i \gamma_i^{(2)}\right) \approx \frac{788730+788730+788494+788494}{10^6} \times 4\pi \times \left(\sqrt{\frac{3}{4}}\right)^2. \tag{C.3}$$

Third, due to symmetry, there is only one 1-sphere (circle) and any point on it lies on all those 3-spheres. This 1-sphere has center $(\frac{1}{2}, \frac{1}{2}, 0, 0)$ and radius $\sqrt{\frac{1}{2}}$, satisfying

$$x_1 = \frac{1}{2}, \quad x_2 = \frac{1}{2}, \quad x_3^2 + x_4^2 = \frac{1}{2}, \tag{C.4}$$

where (x_1, x_2, x_3, x_4) denote the Cartesian coordinates. The length of this 1-sphere is $\sqrt{2}\pi$. Note that there is no intersection point on the boundary of the union of these 4-balls. According to Eq. (3.15), we can finally approximate the volume of Ω as follows

$$\begin{aligned}\mathrm{Vol}^{(4)}(\Omega) &= \frac{1}{4}\mathrm{Vol}^{(3)}\left(\bigcup_i \gamma_i^{(3)}\right) + \frac{1}{6}\mathrm{Vol}^{(2)}\left(\bigcup_i \gamma_i^{(2)}\right) \times \left(\frac{1}{2}\sqrt{\frac{3}{4}}\right) \\ &\quad + \frac{1}{4} \times \sqrt{2}\pi \times \left(\frac{1}{3}\sqrt{\frac{1}{2}}\right) \\ &\approx 14.92.\end{aligned} \tag{C.5}$$

In the above simple example, we have presented how Eq. (3.15) can be used to approximate the volume of the union of d-balls. However, this might not be the most convenient way to approximate the volume. For instance, we can take a box covering Ω and then use the Monte Carlo method with a set of uniformly distributed points in the box. In this case, one no longer needs to consider the k-spheres, but to test whether or not a sampling point is covered by any d-ball. In fact, we have observed that the results from both methods trend to the same value when the number of sampling points increases, which verifies Eq. (3.15). What one effectively gains using Eq. (3.15) is the reduction of 1 dimension, which might be negligible for high dimensions.

REFERENCES

[1] N. Amenta and R. K. Kolluri, *The medial axis of a union of balls*, Computational Geometry, 20 (2001), pp. 25–37.

[2] D. Attali and A. Montanvert, *Computing and simplifying 2d and 3d continuous skeletons*, Computer Vision and Image Understanding, 67 (1997), pp. 261–273.

[3] F. Aurenhammer, *Power diagrams: properties, algorithms and applications*, SIAM Journal on Computing, 16 (1987), pp. 78–96.

[4] D. Avis, B. K. Bhattacharya, and H. Imai, *Computing the volume of the union of spheres*, Visual Computer, 3 (1988), pp. 323–328.

[5] H. M. Berman, J. Westbrook, Z. Feng, G. Gilliland, T. N. Bhat, H. Weissig, I. N. Shindyalov, and P. E. Bourne, *The Protein Data Bank*, Nucleic Acids Research, 28 (2000), pp. 235–242.

[6] H. Bium, *A transformation for extracting new descriptions of shape*, in Symposium on Models for the Perception of Speech and Visual Form, 1964.

[7] F. Cazals, H. Kanhere, and S. Loriot, *Computing the volume of a union of balls: a certified algorithm*, ACM Transactions on Mathematical Software (TOMS), 38 (2011), p. 3.

[8] M. P. Do Carmo and M. P. Do Carmo, *Differential geometry of curves and surfaces*, vol. 2, Prentice-hall Englewood Cliffs, 1976.

[9] R. L. S. Drysdale, III, *Generalized Voronoi Diagrams and Geometric Searching.*, PhD thesis, Stanford University, Stanford, CA, USA, 1979. AAI7917225.

[10] J. Giesen, B. Miklos, and M. Pauly, *Medial axis approximation of planar shapes from union of balls: A simpler and more robust algorithm*, in CCCG, no. EPFL-CONF-149319, 2007, pp. 105–108.

[11] H. Imai, M. Iri, and K. Murota, *Voronoi diagram in the laguerre geometry and its applications*, SIAM Journal on Computing, 14 (1985), pp. 93–105.

[12] A. Lieutier, *Any open bounded subset of rn has the same homotopy type as its medial axis*, Computer-Aided Design, 36 (2004), pp. 1029–1046.

[13] G. Marsaglia, *Choosing a point from the surface of a sphere*, Ann. Math. Statist., 43 (1972), pp. 645–646.

[14] A. Okabe, B. Boots, K. Sugihara, and S. N. Chiu, *Spatial tessellations: concepts and applications of Voronoi diagrams*, vol. 501, John Wiley & Sons, 2009.

[15] F. W. Olver, *NIST handbook of mathematical functions hardback and CD-ROM*, Cambridge University Press, 2010.

[16] C. Quan and B. Stamm, *Mathematical analysis and calculation of molecular surfaces*, Journal of Computational Physics, 322 (2016), pp. 760 – 782.

[17] R. T. Rockafellar, *Convex Analysis, volume 28 of Princeton Mathematics Series*, Princeton University Press, 1970.